DOI: 10.1002/ejic.200600940

Gas-Phase Structure and Vibrational Properties of Trifluoromethyl Trifluoromethanesulfonate, $CF_3SO_2OCF_3$

María E. Tuttolomondo,[a] Pablo E. Argañaraz,[a] Eduardo L. Varetti,[b][‡] Stuart A. Hayes,[c] Derek A. Wann,[c] Heather E. Robertson,[c] David W. H. Rankin,[c] and Aida Ben Altabef*[a][‡]

Keywords: Electron diffraction / IR spectroscopy / Raman spectroscopy / Structure elucidation / Ab initio calculations

Trifluoromethyl trifluoromethanesulfonate, $CF_3SO_2OCF_3$, has been synthesised and its gas-phase structure determined from electron-diffraction data. This structural study was supported by HF, MP2 and DFT (B3LYP and B1B95) calculations, which revealed a strong dependence of the theoretical structure on the polarisation of the basis set. Infrared spectra for the gas and solid and a Raman spectrum for the liquid were obtained, and the observed bands were assigned. The experimental vibrational data, along with theoretical (B3LYP) force constants, were used to define a scaled quantum mechanical force field, which enabled reproduction of the measured frequencies with a final root-mean-square deviation of 6 cm^{-1}.

Introduction

The synthesis of trifluoromethyl trifluoromethanesulfonate, $CF_3SO_2OCF_3$, was first reported by Noftle and Cady[1] as a product of the thermal decomposition of $(CF_3SO_2)_2O$. Different synthetic routes were later proposed by Olah and Ohyama,[2] Kobayashi et al.[3] and Hassani et al.,[4] but no structural or vibrational studies have been reported.

Our previous studies on derivatives of trifluoromethanesulfonic acid[5–8] have been extended to $CF_3SO_2OCF_3$ in order to investigate further the characteristic conformations and force constants for such molecules. For that purpose, the substance has been synthesised and its gas-phase structure determined by electron diffraction. Additionally, infrared and Raman spectra were recorded for different physical states. These experimental measurements were complemented by quantum chemical calculations to obtain an optimised molecular structure and frequencies corresponding to the normal modes of vibration. Of particular interest is the comparison of the experimental and theoretical molecular geometric parameters and conformational isomers with the experimental results previously obtained for $CF_3SO_2OCH_3$[5] and $ClSO_2OCF_3$,[9] and with those calculated for several CF_3SO_2X[6] and CF_3SO_2OX[7,8] molecules, which shows that covalent sulfonates prefer a *gauche* conformation (Figure 1).[5]

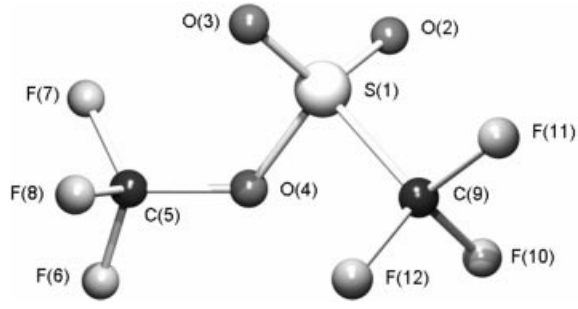

Figure 1. Molecular structure of $CF_3SO_2OCF_3$, showing atom numbering.

Results and Discussion

Theoretical Study

A starting geometry for $CF_3SO_2OCF_3$ was obtained by using RHF theory with a 3-21G(d) basis set[10–12] followed by a 6-31G(d) basis set.[13–15] Electron correlation was then accounted for by using the MP2,[16] B3LYP[17] and B1B95[18] methods before increasing the basis set sequentially from 6-31G(d) to 6-311+G(d).[19,20] In addition, the 6-31G(3df) basis set,[21] the Dunning correlation-consistent basis sets, cc-pVDZ and cc-pVTZ[22] and Ahlrichs' TZVP[23] and TZVPP[24] basis sets were used to gauge the

[a] Instituto de Química Física, Facultad de Bioquímica, Química y Farmacia, Universidad Nacional de Tucumán, San Lorenzo 456, 4000 Tucumán, R. Argentina
E-mail: altabef@fbqf.unt.edu.ar
[b] Centro de Química Inorgánica (CEQUINOR, CONICET-UNLP), Departamento de Química, Facultad de Ciencias Exactas, Universidad Nacional de La Plata, C. Correo 962, 1900 La Plata, R. Argentina
[c] School of Chemistry, University of Edinburgh, West Mains Road, Edinburgh, EH9 3JJ, UK
E-mail: d.w.h.rankin@ed.ac.uk
[‡] Members of the Carrera del Investigador Científico, CONICET, R. Argentina
Supporting information for this article is available on the WWW under http://www.eurjic.org or from the author.

effect of including further polarisation functions. The results of the geometry optimisations are available in Tables S1 and S2 in the Supporting Information. In all cases, a molecular structure with C_1 symmetry was predicted, as shown in Figure 1. The force field obtained at the RHF/6-31G(d) level was then used with the program SHRINK[25] to obtain estimates of the amplitudes of vibration (u_{h1}) and perpendicular vibrational correction terms (k_{h1}) used in the gas electron diffraction (GED) refinement.

Scans of the potential energy with respect to the C–S–O–C torsion were performed at the RHF/6-31G(d) and MP2/6-31G(d) levels and a third scan at the MP2/6-31G(d) level with the 6-31G(3df) basis set on sulfur (Figure 2). These reveal two symmetrically equivalent minima, corresponding to enantiomers, and O–C(5) eclipses one or other of the S=O bonds when viewed down the S–O(4) bond. As enantiomers are indistinguishable by GED, the subsequent refinement was performed with the eclipsing of the S=O(3) bond by O–C as in the calculated structures. The shallow barrier between the two equivalent conformers is ca. 5–10 kJ mol^{-1}, easily surmountable at the experimental temperatures. The quantum chemical calculations predict the existence of two stable, asymmetric (point group C_1) and structurally equivalent conformers for $CF_3SO_2OCF_3$, both with a *gauche* conformation with a C–S–O–C dihedral angle of about 110°. As shown in Table 1, this angle is relatively sensitive to changes in method and basis set and has a larger value than that calculated for $CF_3SO_2OCH_3$ (93°).[5] Similar molecules that were previously studied by us were also calculated to have *gauche* conformations, with C–S–O–C dihedral angles of 114.8° in $CF_3SO_2OCH_2CF_3$[7] and 91.5° in $CF_3SO_2OCH_2CH_3$[8] [B3LYP/6-31G(d) values in both cases].

The calculated C–O and C–F bond lengths converged reasonably well with increasing basis set size and showed fairly good agreement between different post-Hartree–Fock methods, as shown in Table 1. Bond lengths to sulfur, however, are extremely sensitive to both method and basis set. Particularly interesting was the result of adding additional polarisation functions to the basis set, which resulted in shortening of the bond lengths, the most significant is a reduction of 5.5 pm for the S–O bond [MP2/6-31G(d) to MP2/6-31G(3df)].

With reference to structural studies on $CF_3SO_2OCH_3$[5] and $ClSO_2OCF_3$,[9] the bond lengths to sulfur were overestimated by B3LYP relative to those obtained by GED and X-ray crystal values (the latter for $ClSO_2OCF_3$ only). With this in mind, the MP2/6-31G(3df) geometry appeared to be the best as both a starting point for the GED refinement and the basis for geometrical restraints.

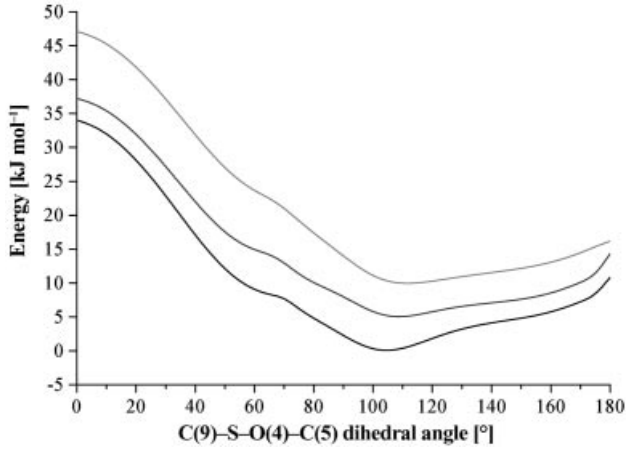

Figure 2. Torsional potential around the S–O(4) bond for $CF_3SO_2OCF_3$, stepped in 5° increments. Calculations were performed at the HF (light grey) and MP2 (dark grey) levels by using a 6-31G(d) basis set and by using MP2/6-31G(d) with 3df polarisation on sulfur (black).

GED Model

The molecular model for the GED refinement assumed overall C_1 symmetry (Figure 1), as predicted by the calculations. The structure of $CF_3SO_2OCF_3$ was defined in terms of 25 independent parameters, comprising 11 bond lengths and differences, 10 bond angles and differences, one tilt angle and three torsional angles, listed in Table 2. The bonded distances S–O(4), O(4)–C(5) and S–C(9) were each defined individually (p_7, p_{10} and p_{11}, respectively), whilst simple averages were taken of the six C–F bond lengths (p_1) and of the two S=O bond lengths (p_8). The difference between the average C–F distance in the CF_3 group bonded to O(4) (group 1) and the average C–F distance in the CF_3 group bonded directly to the sulfur atom (group 2) was defined (p_2). For CF_3 in group 1, the C–F(6) distance was then found by defining the difference between this distance and the average of the C–F(7) and C–F(8) bond lengths (p_3). The difference between the latter two bond lengths was then defined (p_5). Similarly, in group 2, the difference between the C–F(11) distance and an average of the other two bond lengths (p_4) and the difference between the C–F(12) bond length and the C–F(10) bond length (p_6) were defined. The

Table 1. Selected calculated and GED geometrical parameters for $CF_3SO_2OCF_3$ (distances in pm, angles in °).

	GED	HF/ 6-31G(d)	MP2/ 6-31G(d)	6-311+G(d)	6-31G(3df)	cc-pVTZ	TZVPP	B3LYP/ 6-31G(3df)	B1B95/ 6-31G(3df)
*r*C–F average	133.3(2)	130.2	133.3	132.5	131.9	132.1	132.1	132.6	131.8
*r*S–O	161.5(4)	160.3	167.7	167.1	162.2	163.9	163.8	163.6	161.8
*r*S=O average	141.9(3)	140.9	144.7	143.4	141.9	143.1	143.1	142.0	141.4
*r*C–O	139.3(7)	137.4	139.3	138.5	139.0	139.1	139.0	139.5	138.9
*r*C–S	181.3(4)	182.1	184.5	186.3	183.8	185.4	185.6	187.4	185.1
ϕC–S–O–C	119.5(18)	111.2	108.4	110.7	105.6	108.2	108.6	105.8	107.5

difference between the two S=O double bond lengths (p_9) allowed these bond lengths to be defined.

Table 2. GED refined parameters (r_{h1} structure) for $CF_3SO_2OCF_3$ (distances in pm, angles in degrees).

	Description	Value	MP2/6-31G(3df)	Restraint uncertainty[a]
	Independent parameters			
p_1	*r*C–F average	133.3(2)	131.9	
p_2	*r*C–F difference 1	–0.4(1)	–0.4	0.1
p_3	*r*C–F difference 2	0.4(1)	0.4	0.1
p_4	*r*C–F difference 3	0.2(1)	0.2	0.1
p_5	*r*C–F difference 4	0.2(1)	0.2	0.1
p_6	*r*C–F difference 5	0.0(1)	0.0	0.1
p_7	*r*S–O	161.5(4)	162.2	
p_8	*r*S=O average	141.9(3)	141.9	
p_9	*r*S–O difference	0.4(1)	0.4	0.1
p_{10}	*r*C–O	139.3(7)	139.0	
p_{11}	*r*C–S	181.3(4)	183.8	
p_{12}	∠O(4)–S–C	96.9(10)	97.0	1.0
p_{13}	∠O–S–O(4) average	108.0(2)	108.0	
p_{14}	∠O–S–O(4) difference	3.8(4)	4.4	0.5
p_{15}	∠C–S–O average	107.9(3)	107.6	
p_{16}	∠C–S–O difference	1.3(2)	1.3	0.2
p_{17}	∠S–O–C	121.8(4)	121.3	0.5
p_{18}	∠O–C–F(6)	104.6(4)	105.8	
p_{19}	∠F–C–F group 1 average	108.0(2)	109.3	
p_{20}	∠F–C–F group 1 difference	0.3(2)	0.4	0.2
p_{21}	∠S–C–F tilt	1.6(5)	1.6	0.5
p_{22}	∠F–C–F group 2	108.6(2)	109.8	
p_{23}	ϕC–S–O–C	119.5(18)	105.6	
p_{24}	ϕS–O–C–F(6)	195.2(9)	182.6	
p_{25}	ϕO–S–C–F(11)	177.2(10)	178.5	2.0
	Dependent parameter			
d_1	∠O(2)=S=O(3)	124.6(8)	125.1	1.0

[a] Restraint values are given by the corresponding MP2/6-31G(3df) values.

The geometry around sulfur was described using three angles and two differences: the O(4)–S–C(9) angle (p_{12}), the average of the O(2)–S–O(4) and O(3)–S–O(4) angles (p_{13}) and their difference (p_{14}), and the average of the O(2)–S–C(9) and O(3)–S–C(9) angles (p_{15}) and their difference (p_{16}).

Fluorine atom positions in CF_3 in group 1 were described by using the average of the three internal F–C–F angles (p_{19}) and the difference between the F(7)–C–F(8) angle and the angles F(6)–C–F(7) and F(6)–C–F(8) (p_{20}), the latter two angles are assumed to be identical. The orientation of this CF_3 group with respect to sulfur was defined by using the angles S–O–C (p_{17}) and O–C–F(6) (p_{18}), and the torsional angles C–S–O–C (p_{23}) and S–O–C–F(6) (p_{24}).

CF_3 in group 2 was described by using a single F–C–F angle (p_{22}) and orientated by using a tilt angle (p_{21}). A positive tilt was defined as a reduction in the S–C–F(11) angle, with the zero point occurring when the three S–C–F angles are equal. This group was also allowed to rotate around the S–C bond, defined by the torsional angle O(4)–S–C–F(11) (p_{25}). In this case, an angle of 180° corresponds to a staggered conformation and a larger angle brings F(11) closer to O(3).

Electron Diffraction Refinement

The GED refinement (Table 3) was carried out with the SARACEN method,[26] which allows parameters that are poorly defined by GED data alone to be restrained to calculated values with specified uncertainties, on the basis of the degree of convergence of the calculations. Distances were corrected for curvilinear perpendicular motion (k_{h1}) and yielded r_{h1} parameters.[25] All 25 independent parameters were refined, along with two individual and eight groups of amplitudes of vibration, to produce an R_G factor of 0.067 (R_D = 0.029). The refined parameters are displayed in Table 2 along with the corresponding values predicted by MP2/6-31G(3df) calculations. The radial-distribution curve is shown in Figure 3, and the molecular-scattering intensity curve is provided as Supporting Information (Figure S1).

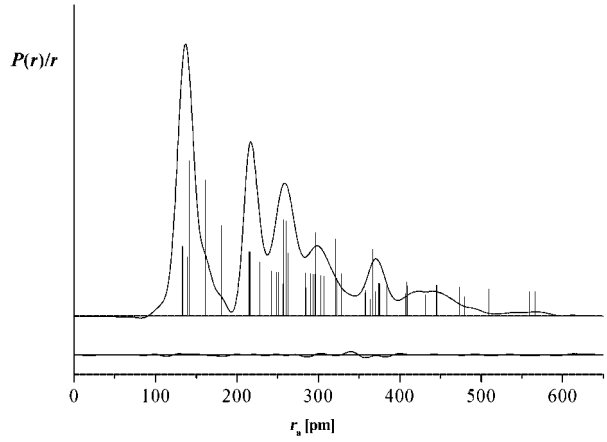

Figure 3. Experimental and difference (experimental – theoretical) radial-distribution curves, $P(r)/r$, for $CF_3SO_2OCF_3$. Before Fourier inversion, the data were multiplied by $s \times \exp[(-0.00002s^2)/(Z_S - f_S)(Z_F - f_F)]$.

Where required, restraints on geometrical parameters were derived from the MP2/6-31G(3df) calculated values. Those applied directly to independent or dependent parameters are given in Table 2, whilst restraints on the differences between independent parameters are provided in Table 3. The only group of amplitudes of vibration allowed to refine

Table 3. Restraints on differences between pairs of independent parameters (distances in pm, angles in degrees).

Difference		GED[a]	MP2/6-31G(3df)	Uncertainty[b]
$p_{10} - p_1$	[*r*C–O] – [*r*C–F average]	6.1(8)	7.0	1.0
$p_{13} - p_{15}$	[∠O–S–O(4) average] – [∠C–S–O average]	0.1(2)	0.3	0.2
$p_{22} - p_{19}$	[∠F–C–F group 2] – [∠F–C–F group 1 average]	0.5(2)	0.5	0.2
$p_{19} - p_{18}$	[∠F–C–F group 1 average] – [∠O–C–F(6)]	3.5(5)	3.5	0.5

[a] Refined value. [b] Restraint values are given by the corresponding MP2/6-31G(3df) values.

unrestrained was that containing the bonded distances of less than 150 pm. The remaining amplitudes for bonded atom pairs were restrained with uncertainties of 10% of their calculated values, whilst the groups of non-bonded amplitudes were restrained with uncertainties of 20%. A full list of interatomic distances and corresponding calculated and refined amplitudes of vibration are provided in Table S3 (Supporting Information), and the least-squares correlation matrix in Table S4.

GED and Calculated Structures

Two large discrepancies can be seen between the GED and calculated structures: the S–C bond length and the torsional angles, particularly C–S–O–C. The S–C distance is 2.5 pm shorter than that predicted by MP2/6-31G(3df) calculations. However, the S–O bond length, which for similar compounds is generally poorly defined by theory, is only 0.7 pm shorter experimentally. The MP2/6-31G(3df) calculation is thus significantly more accurate for predicting these bond lengths than other methods or basis sets requiring similar computational resources. For instance, the MP2/6-311+G(d) calculation overestimates the S–O and S–C distances by 5.6 and 3.0 pm, respectively, and B3LYP/6-31G(3df) underestimates the same bond lengths by 2.0 and 6.1 pm, respectively. The B1B95/6-31G(3df) calculation predicts parameter values that are similar to those predicted by MP2, overestimating the respective S–O and S–C distances by 0.3 and 3.8 pm, respectively, relative to the GED values. MP2 and B1B95 are therefore marginally better than B3LYP at describing the geometry of $CF_3SO_2OCF_3$, and for this type of compound, B1B95 is likely be the best compromise between accuracy and computational cost. Comparison of these results with parameters for similar compounds $CF_3SO_2OCH_3$[5] and FSO_2OSF_5,[27] studied by GED and B3LYP/6-31G(d) calculations, shows that in these cases, despite the reasonably close agreement between different theoretical methods, the experimental S–O bonds are 5–7 pm shorter. In the case of $CF_3SO_2OCH_3$,[5] the experimentally determined S–C bond is 3.3 pm shorter. The study on $ClSO_2OCF_3$[9] also shows that B3LYP/6-311G(d) underestimates the S–O bond length by 6 to 7 pm, but the B3LYP/6-311+G(3df) calculation reduces this difference to ca. 3 pm. These GED and theoretical results are therefore consistent with the more general observation that distances between sulfur and oxygen are poorly predicted with standard methods [such as MP2/6-31G(d)], and indicate that this may be due primarily to insufficient polarisation functions in the basis set. This conclusion is also consistent with the molecular structures calculated at the MP2 level by using Dunning's cc-pVDZ and cc-pVTZ, and Ahlrichs' TZVP and TZVPP basis sets (Table S2). As was the case for the Pople 6-31G(d) basis set, the cc-pVDZ and TZVP bases contain only a single d-type Gaussian and underestimate the S–O bond length by 8.9 and 6.6 pm, respectively. In contrast, the cc-pVTZ and TZVPP bases, which both incorporate two d-type and one f-type Gaussian, underestimate the S–O bond length by just 2.4 and 2.3 pm, respectively, relative to the GED determined value of 161.5(4) pm. Similar observations can also be made for the S=O and S–C bond lengths, albeit to a lesser extent.

The C–S–O–C torsional angle was found to be 119.5(18)° by GED relative to between 105 and 112° by various theoretical methods. However, the estimated standard deviation of this value does not give a good estimate of its uncertainty, as the refinement can be performed by fixing this angle at any arbitrary value between 100 and 150° without significantly affecting the remaining parameters or the R_G factor. It would, in principle, be possible to replace the rigid model adopted in the refinement by a dynamic model based on the potential function of the C–S–O–C torsion. However, it can be seen from the theoretical potential energy scan (Figure 2) that this potential energy curve is not a simple function, and several parameters would be required to model it. In such cases, the uncertainties of the extra parameters are extremely large, and so the refined values are of little physical significance. We therefore did not use such a dynamic model in this case.

Vibrational Study

$CF_3SO_2OCF_3$ has C_1 symmetry, and therefore its 30 normal modes of vibration are active in the IR and Raman spectra. Representative spectra appear in Figures 4 (IR spectra of the gas and solid) and 5 (Raman spectrum of the liquid), and the frequencies for the observed spectral features are collated in Table 4.

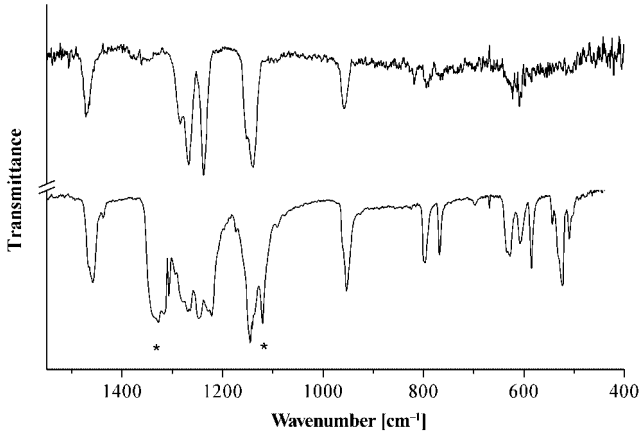

Figure 4. Infrared spectra for $CF_3SO_2OCF_3$ in the gas phase (upper trace; resolution 2 cm^{-1}, path length 10 cm, pressure ca. 1.0 Torr) and in the solid phase (lower trace; film on cooled KBr window, resolution 2 cm^{-1}). Asterisks indicate solid SO_2 bands.

The B3LYP calculations reproduced the normal frequencies of vibration with the following root-mean-square-deviation (RMSD) values for each basis set: 19.8 cm^{-1} for 6-31G(d), 21.6 cm^{-1} for 6-311G(d) and 27.1 cm^{-1} for 6-311+G(d). The first and second basis sets reproduce the experimental frequencies somewhat better, and the results obtained with the 6-31G(d) basis set were used for the vibrational analysis, in order to allow direct comparison with

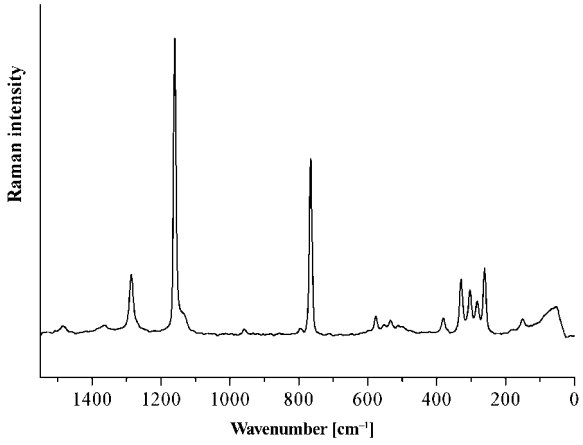

Figure 5. Raman spectrum for liquid $CF_3SO_2OCF_3$ (resolution 4 cm^{-1}).

Table 4. Frequencies of observed bands in the infrared and Raman spectra of $CF_3SO_2OCF_3$ (units are cm^{-1}).[a]

Infrared		Raman[b]	Mode assignment
Gas	Solid	Liquid	
1469 (s)	1458 (s)	1458 (3)	ν_1
		1342 (3)	?
	1327 (vs)		SO_2
1282 (s)	1277 (s)		ν_2
1268 (vs)	1268 (vs)	1268 (20)	ν_3
	1266 (vs)		ν_4
1236 (vs)	1246 (vs)		ν_5, ν_6
	1228 (s)		
	1221 (vs)		
1150 (sh.)	1144 (vs)	1146 (100)	ν_7
1139 (vs)	1140 (vs)		ν_8
	1119 (s)		SO_2
956 (s)	952 (s)	952 (2)	ν_9
816 (m)			?
792 (m)	796 (m)	794 (2)	ν_{10}
766 (w)	767 (m)	766 (60)	ν_{11}
	695 (vw)		ν_{12}
627 (m)	628 (m)		ν_{13}
606 (m)	606 (m)	603 (vvw)	ν_{14}
586 (w)	584 (m)	584 (6)	ν_{15}
		560 (3)	ν_{16}
540 (vw)	542 (w)	542 (5)	ν_{17}
	522 (m)	520 (3)	?
508 (w)	508 (w)	509 (3)	ν_{18}
	444 (vvw)	445 (vvw)	ν_{19}
		394 (9)	ν_{20}
		345 (19)	ν_{21}
		320 (15)	ν_{22}
		300 (11)	ν_{23}
		280 (23)	ν_{24}
		200 (1, br.)	ν_{25}
		172 (4)	ν_{26}
		150 (sh.	ν_{27}

[a] s = strong, m = medium, w = weak, v = very, sh. = shoulder, br. = broad. [b] For the Raman spectrum, relative band heights are given in parentheses.

calculations performed previously for related molecules. The calculated frequencies of vibration appear in Table 5, together with the experimental values.

The proposed assignments of spectral features to the different modes of vibration given in Table 4 are based on the calculated frequencies and on the infrared and Raman intensities and also on comparisons with known data for related molecules.

SO_2 Group Modes

The SO_2 antisymmetric and symmetric stretching modes appear in the regions 1357–1467 cm^{-1} and 1140–1157 cm^{-1}, respectively, in the molecules CF_3SO_2X (X = F, OH, NH_2, CH_3, OCH_2CH_3, OCH_2CF_3).[6–8] The intense bands observed at 1469 and 1139 cm^{-1} in the spectrum of the gas can therefore immediately be assigned to these modes. The last mode, however, is a complex mix of several simple vibrations, as discussed below. The medium intensity band at 586 cm^{-1} in the gas infrared spectrum is assigned to the SO_2 bend. This frequency is somewhat higher than usual, as this mode appears in the region 488–538 cm^{-1} in the compounds listed above. The bands for the three modes corresponding to the movements of the whole SO_2 group appear at relatively low frequencies. The following assignments are proposed, with the corresponding frequency ranges for the molecules mentioned above in parentheses: SO_2 wagging, 606 cm^{-1} (611–628 cm^{-1}); SO_2 rocking, 394 cm^{-1} (382–463 cm^{-1}); SO_2 twisting, 300 cm^{-1} (310–351 cm^{-1}). These assignments are also supported by the calculations.

Trifluoromethyl Group Modes

Inspection of the atomic displacements for the vibrational modes calculated in the 1100–1300 cm^{-1} region shows that the stretching vibrations, especially the symmetric stretches, of the two CF_3 groups are strongly coupled. For this reason it is not possible to discuss the assignments of bands for these two groups separately.

The two CF_3 symmetric modes are predicted to have large Raman intensities. One mode includes the symmetric stretches of the two CF_3 groups, coupled with contributions from the CS and CO stretches and the SO_2 symmetric stretch; the latter is out of phase in relation to the other four. The second mode mixes the same five simple vibrations, but with the SO_2 symmetric stretch now in phase. These two complex modes are assigned to the strong Raman bands located at 1268 and 1146 cm^{-1}. The 1146 cm^{-1} band exhibits a shoulder at ca. 1120 cm^{-1}, best defined in the infrared spectrum of the solid, and is assigned to a third mode, which also mixes the two CF_3 symmetric stretching vibrations and the CO and CS stretches in an out-of-phase fashion, but with almost no participation of the SO_2 symmetric stretch. Four bands should still be assigned to the CF_3 antisymmetric stretching vibrations. As not enough arguments are available for precise assignments, those appearing in Table 4 and Table 5 are tentative.

Symmetric deformation modes are observed at 792 cm^{-1} (CF_3S group) and 695 cm^{-1} (CF_3O group) in the gas infrared spectra. The two antisymmetric deformation modes of the SCF_3 group appear at 540 and 560 cm^{-1}, i.e. about 10 cm^{-1} higher than the calculated values. The antisymmet-

Table 5. Observed and calculated frequencies, infrared and Raman intensities and potential-energy distribution for $CF_3SO_2OCF_3$.

Mode	Observed	Calculated[a]	Calculated SQM[b]	IR intensity[c]	Raman activity[d]	Potential-energy distribution[e]
1	1469	1414	1461	287	3.6	$96S_1$
2	1282	1304	1283	48	9.1	$54S_2 + 20S_8 + 11S_{21}$
3	1268	1242	1272	308	0.86	$31S_2 + 10S_7 + 25S_8$
4	1266	1293	1263	212	0.52	$30S_4 + 10S_5 + 51S_6 + 12S_{13} + 11S_{19}$
5	1236	1283	1247	334	0.64	$51S_4 + 40S_5$
6	1236	1264	1233	515	2.1	$16S_4 + 46S_5 + 31S_6$
7	1150	1116	1152	238	6.4	$21S_3 + 31S_7 + 29S_9 + 22S_{10} + 24S_{12} + 13S_{22}$
8	1139	1144	1142	280	2.2	$15S_3 + 12S_7 + 44S_8 + 36S_9 + 20S_{12}$
9	956	933	937	137	1.0	$28S_3 + 31S_9 + 23S_{11}$
10	792	777	795	26	1.5	$37S_7 + 17S_{10} + 14S_{22}$
11	766	737	756	105	16.0	$21S_3 + 39S_{11} + 12S_{21}$
12	695	682	696	3.87	0.53	$12S_3 + 24S_{12} + 15S_{26}$
13	627	613	634	66	0.47	$12S_6 + 12S_{13} + 19S_{14} + 19S_{19}$
14	606	588	610	114	0.60	$12S_{10} + 12S_{12} + 16S_{13} + 30S_{14}$
15	586	567	589	38	3.0	$38S_{15} + 10S_{17}$
16	560	549	559	0.37	2.2	$54S_{16}$
17	540	526	536	29	2.9	$45S_{17} + 17S_{18}$
18	508	487	502	20	1.3	$19S_{15} + 12S_{17} + 49S_{18}$
19	444	430	453	1.90	0.17	$49S_{13} + 57S_{19}$
20	394	380	397	3.94	2.2	$21S_{16} + 36S_{20} + 21S_{25}$
21	345	325	341	1.05	4.8	$18S_{11} + 28S_{15} + 25S_{21} + 14S_{27}$
22	320	304	319	1.05	3.6	$10S_{11} + 12S_{14} + 14S_{21} + 17S_{22} + 16S_{24}$
23	300	275	289	1.37	2.6	$39S_{23} + 17S_{25}$
24	280	263	277	5.50	3.8	$23S_{22} + 36S_{24}$
25	200	185	195	2.03	0.25	$34S_{20} + 49S_{23} + 56S_{25}$
26	172	158	170	1.07	0.44	$56S_{56} + 23S_{27}$
27	150	145	154	1.31	0.26	$28S_{24} + 19S_{26} + 86S_{27} + 12S_{28} + 15S_{29}$
28	–	66	67	0.15	0.04	–
29	–	51	51	0.15	0.01	–
30	–	36	36	0.03	0.01	–
RMSD		19.8	6.04			

[a] B3LYP/6-31G* calculation. Observed and calculated values in cm^{-1}. [b] From scaled quantum mechanics force field (see text for further definition). [c] Units are km mol^{-1}. [d] Units are Å^4(amu)$^{-1}$. [e] See Table 6 for definitions of natural symmetry coordinates.

ric deformation modes of the CF_3O group show a larger splitting, appearing at 508 and 627 cm^{-1}.

The CF_3 rocking modes were assigned by taking into account the theoretically predicted frequencies and with knowledge of modes in related molecules. In this way, the weak bands located at 200 and 280 cm^{-1} are assigned to the rocking modes of the CF_3S group, which appear at around 200 and 340 cm^{-1} in CF_3SO_2X molecules.[6] Higher frequencies, with values of 340 and 440 cm^{-1}, were reported for the CF_3O rocking motions in CF_3OX molecules,[28] and consequently the bands observed at 345 and 444 cm^{-1} for $CF_3SO_2OCF_3$ are assigned to these modes.

Skeletal Modes

The O–S stretching mode appears as a strong Raman band located at 766 cm^{-1}. The strong 956 cm^{-1} infrared band in the gas spectrum is well predicted by calculations, in terms of both position and intensity, to be due to the C–O stretch, although the mode is best described as the out-of-phase coupling of the C–O and O–S stretches, as can be observed from the calculated atomic displacements when displayed with the program GaussView.[29]

The 320 cm^{-1} mode shows a strong contribution from the C–S stretch. The CSO bend appears as the main component of the 150 cm^{-1} mode, and is also strongly coupled with the COS bend in the 172 cm^{-1} mode. These last two modes appear as very weak, ill-defined Raman bands.

Torsional Modes

Very weak spectral features were expected for the three torsional modes and, in fact, no bands could be identified to be assigned to these modes.

Calculation of Force Constants

The Cartesian force field for $CF_3SO_2OCF_3$, as calculated, was transformed into the set of non-redundant, natural coordinates defined in Table 6 through the B-matrix[30] obtained with a standard program. Such coordinates take into account the local symmetry around the C and S atoms and are in accordance with the proposals of Fogarasi et al.[31] The resulting force field was subsequently scaled by using the scheme proposed by Pulay et al.,[32] in which the diagonal force constants are multiplied by scale factors $k_{f,i}$, $k_{f,j}$, etc., and the corresponding interaction constants are multiplied by $(k_{f,i} \times k_{f,j})^{1/2}$. A set of initial scale factors was defined by using values recommended by Kalincsák and Pongor[33] where available and by using unity for the rest. These scale factors were subsequently adjusted by a least-squares procedure in order to obtain the best fit to the experimental frequencies.(initial and final scale factors are available in Table S5, Supporting Information). All vibrational bands were assigned the same weight in the adjustment except for those missing or showing uncertain fre-

Table 6. Definitions of natural symmetry coordinates for $CF_3SO_2OCF_3$.[a]

Label	Definition	Description
S_1	r(1–2) – r(1–3)	SO_2 antisymmetric stretch
S_2	2m(6–5) – m(8–5) – m(7–5)	OCF_3 antisymmetric stretch
S_3	m(8–5) + m(6–5) + m(7–5)	OCF_3 symmetric stretch
S_4	d(9–10) – d(9–12)	SCF_3 antisymmetric stretch
S_5	2d(9–11) – d(9–10) – d(9–12)	SCF_3 antisymmetric stretch
S_6	m(8–5) – m(7–5)	OCF_3 antisymmetric stretch
S_7	d(9–10) + d(9–11) + d(9–12)	SCF_3 symmetric stretch
S_8	r(1–2) + r(1–3)	SO_2 symmetric stretch
S_9	p(4–5)	C–O stretch
S_{10}	ε(10–9–11) + ε(10–9–12) + ε(11–9–12) – β(10–9–1) – β(11–9–1) – β(12–9–1)	SCF_3 symmetric bend
S_{11}	l(1–4)	S–O stretch
S_{12}	μ(6–5–7) + μ(6–5–8) + μ(7–5–8) – Ω(6–5–4) – Ω(7–5–4) – Ω(8–5–4)	OCF_3 symmetric bend
S_{13}	μ(8–5–6) – μ(7–5–6)	OCF_3 antisymmetric bend
S_{14}	ψ(9–1–2) + ψ(9–1–3) – γ(4–1–2) – γ(4–1–3)	SO_2 wag
S_{15}	4φ(2–1–3) – ψ(9–1–2) – ψ(9–1–3) – γ(4–1–2) – γ(4–1–3)	SO_2 bend
S_{16}	ε(10–9–11) – ε(12–9–11)	SCF_3 antisymmetric bend
S_{17}	2ε(10–9–12) – ε(10–9–11) – ε(12–9–11)	SCF_3 antisymmetric bend
S_{18}	2μ(8–5–7) – μ(8–5–6) – μ(7–5–6)	OCF_3 antisymmetric bend
S_{19}	Ω(8–5–4) – Ω(7–5–4)	CF_3 rock
S_{20}	ψ(9–1–2) – ψ(9–1–3) + γ(4–1–2) – γ(4–1–3)	SO_2 rock
S_{21}	2Ω(6–5–4) – Ω(8–5–4) – Ω(7–5–4)	OCF_3 rock
S_{22}	t(1–9)	C–S stretch
S_{23}	ψ(9–1–2) – ψ(9–1–3) – γ(4–1–2) + γ(4–1–3)	SO_2 twist
S_{24}	2β(11–9–1) – β(10–9–1) – β(12–9–1)	SCF_3 rock
S_{25}	β(10–9–1) – β(12–9–1)	SCF_3 rock
S_{26}	α(1–4–5)	SOC bend
S_{27}	4θ(9–1–4) – ψ(9–1–2) – ψ(9–1–3) – γ(4–1–2) – γ(4–1–3)	CSO bend
S_{28}	τ(9–1–4–5) + τ(2–1–4–5) + τ(3–1–4–5)	S–O torsion
S_{29}	τ(8–5–4–1) + τ(6–5–4–1) + τ(7–5–4–1)	OCF_3 torsion
S_{30}	τ(10–9–1–2) + τ(11–9–1–2) + τ(12–9–1–2) + τ(10–9–1–3) + τ(11–9–1–3) + τ(12–9–1–3) + τ(10–9–1–4) + τ(11–9–1–4) + τ(12–9–1–4)	SCF_3 torsion

[a] Latin letters denote changes in bonds between the atoms whose numbers appear in parentheses. Greek letters denote changes in angles defined by the atoms that are also indicated with numbers.

quencies, for which zero weights were used. No empirical correction of the theoretical geometry was used. The potential-energy distribution, which shows the relative contribution of the diagonal force constants to each vibrational mode, was subsequently calculated with the resulting scaled quantum mechanics (SQM) force field. The resulting frequencies, final RMSD value and potential-energy distribution are presented in Table 5. It can be seen that only about one half of the modes have a participation of ≥50% of one definite coordinate, whereas the other modes represent complex vibrations where several coordinates are involved.

The force-field transformation, scaling and potential-energy distribution calculations were performed with the program FCARTP.[34] The atomic displacements, given by the calculations for each vibrational mode, served as a tool to help understand qualitatively the nature of the molecular vibrations. The program GaussView was used along with the corresponding data to represent this graphically.[29]

The SQM force field (Table S6, Supporting Information) was used to calculate the internal force constants for $CF_3SO_2OCF_3$ (Table 7), and these are compared to the equivalent values for some related molecules. It can be seen that on moving from $CF_3SO_2OCF_3$ to $CF_3SO_2OCH_3$, the calculated S–O bond becomes shorter (from 168.2 to 162.2 pm), and, consequently, the corresponding force constant increases (from 3.82 to 4.96 mdyn Å^{-1}). In contrast, the adjacent O–C bond length increases (from 139.3 to 145.5 pm), and its force constant decreases (from 5.50 to 4.60 mdyn Å^{-1}). The highly electronegative CF_3 group seems to enhance the participation of the oxygen electronic charge in the O–C bond of $CF_3SO_2OCF_3$, strengthening that bond to the detriment of the S–O bond.

Table 7. Force constants in internal (valence) coordinates for $CF_3SO_2OCF_3$ and related molecules.

Force constants[a]	$CF_3SO_2OCF_3$	$CF_3SO_2OCH_3$[b]	$CF_3SO_2OCH_2CF_3$[c]
k_f [C(1)–F]	6.50	5.94	5.85
k_f [C(9)–F]	6.13		6.15
k_f [C–S]	3.00	3.10	3.18
k_f [S–O]	3.82	4.96	4.62
k_f [S=O]	11.05	10.70	10.90
k_f [O–C]	5.50	4.60	5.01
k_f [O = S=O]	1.14	1.19	1.10
k_f [O–S=O]	1.26	1.26	1.25
k_f [C–S–O]	1.16	1.16	1.0
k_f [C–S=O]	1.00	1.00	1.0
k_f [F–C(1)–F]	1.24	1.29	1.29
k_f [F–C(9)–F]	1.36		1.35
k_f [C–F/C–F]	0.94	0.71	0.71
k_f [S=O/S=O]	–0.093	–0.076	–0.076

[a] Units are mdyn Å^{-1} for stretches and stretch–stretch interactions, and mdyn Å rad^{-2} for angular deformations. [b] Ref.[5] [c] Ref.[7]

Conclusions

$CF_3SO_2OCF_3$ was synthesised in good yields by using a published technique. A complete investigation of its gas-phase molecular structure was carried out by using electron diffraction techniques complemented by theoretical methods. The experimental and theoretical structures both show this molecule as a single *gauche* conformer having a C–S–O–C dihedral angle of 119.5(18)° determined by GED, relative to 105 to 112° calculated by quantum chemistry calculations. A comparison of the bond lengths obtained by GED and those predicted by various ab initio and DFT methods shows that $CF_3SO_2OCF_3$ is a particularly challenging case for theoretical geometry optimisation. The inclusion of multiple polarisation functions in the basis set plays a crucial role, but the choice of method is also significant. These results are consistent with what seem to be common structural characteristics of covalent sulfonates.

Infrared and Raman spectra were obtained for $CF_3SO_2OCF_3$, and bands assignable to 27 out of the expected 30 normal modes of vibration were observed. The vibrational data were used as a basis to define the symmetry (SQM force field) and internal force constants of the molecule.

Synthesis

$CF_3SO_2OCF_3$ was synthesised by reaction between CF_3SO_2OH and its anhydride, $(CF_3SO_2)_2O$, according to the method reported by Hassani et al.[4] The reactants were heated in a sealed tube for 1 h at approximately 450 K, and after the reaction had occurred, the product was purified by distillation on a vacuum line.

Gas Electron Diffraction (GED)

Data were collected by using the Edinburgh gas electron diffraction apparatus[35] with an accelerating voltage of ca. 40 kV (ca. 6 pm electron wavelength) on Kodak Electron Image film. Nozzle-to-film distances were determined by using benzene vapour as a standard, immediately after recording the diffraction patterns for $CF_3SO_2OCF_3$. Sample and nozzle temperatures of 195 and 298 K, respectively, were used for both the short and long nozzle-to-camera distances (130.5 and 291.5 mm). The electron scattering pattern was converted into digital form by using an Epson Expression 1680 Pro flatbed scanner with a scanning program that was described elsewhere.[36] Data reduction and least-squares refinements were carried out with the ed@ed program[37] employing the scattering factors of Ross et al.[38] The scale factors, *s* limits, weighting points, correlation parameters and electron wavelengths are given in Table S7 (Supporting Information).

Infrared and Raman Spectra

Infrared spectra for $CF_3SO_2OCF_3$ in the gas and solid phases were recorded in the 400–4000 cm^{-1} range by using a Perkin–Elmer 1600 FTIR instrument. The spectrum for the solid was obtained after depositing the compound from the vacuum line onto a KBr window, maintained at about 197 K, in a variable temperature RIIC (VLT-2) cell. The Raman spectrum for the liquid at room temperature was obtained with the FRA-106 accessory mounted on a Bruker IFS66 FTIR instrument, by using 1064-nm light from a Nd/YAG laser for excitation.

Computational Resources

The majority of the calculations described in this paper were performed with a Linux 10-processor Parallel Quantum Solutions (PQS) workstation[39] running the Gaussian 03 suite of programs.[40] The scans of the potential-energy surface and all calculations using the 6-31G(3df), cc-pVTZ, TZVP and TZVPP basis sets were performed with the resources of the EPSRC National Service for Computational Chemistry Software[41] on a cluster of 22 Linux Opteron nodes, where each Opteron server has twin 2.4 GHz Opteron 250 CPUs and 8 GB of memory connected with a high-speed, low-latency Myrinet network.

Supporting Information (see footnote on the first page of this article): Details of GED data analysis parameters, interatomic distances, amplitudes of vibrations, distance corrections for perpendicular motion, the least-squares correlation matrix and the molecular-scattering intensity curves used in the GED refinement are presented. Geometric molecular parameters for all ab initio and DFT calculations are also given. GED atomic coordinates and those obtained from MP2/6-31G(3df), MP2/cc-pVTZ, MP2/TZVPP, B3LYP/6-31G(3df) and B1B95/6-31G(3df) calculations are provided, as well as the force field scaling factors.

Acknowledgments

Research grants from the following Argentine institutions are gratefully acknowledged: CONICET (Consejo Nacional de Investigaciones Científicas y Técnicas), ANPCYT (Agencia Nacional de Promoción Científica y Tecnológica) (PICT 11127), CIUNT (Consejo de Investigaciones de la Universidad Nacional de Tucumán) and UNLP (Universidad Nacional de La Plata). D. A. W. and H. E. R. thank the EPSRC (grant EP/C513649) and S. A. H. thanks the School of Chemistry, University of Edinburgh for funding.

[1] R. E. Noftle, G. Cady, *Inorg. Chem.* **1965**, *4*, 1010.
[2] G. A. Olah, T. Ohyama, *Synthesis* **1976**, 319.
[3] Y. Kobayashi, T. Yoshida, I. Kumadaki, *Tetrahedron Lett.* **1979**, *20*, 3865.
[4] M. O. Hassani, A. Germain, D. Brunel, A. Commeyras, *Tetrahedron Lett.* **1981**, *22*, 65.
[5] F. Trautner, A. Ben Altabef, L. E. Fernández, E. L. Varetti, H. Oberhammer, *Inorg. Chem.* **1999**, *38*, 3051.
[6] L. E. Fernández, A. Ben Altabef, E. L. Varetti, *J. Mol. Struct.* **2002**, *612*, 1.
[7] M. E. Tuttolomondo, L. E. Fernández, A. Navarro, E. L. Varetti, A. Ben Altabef, *Spectrochim. Acta Part A* **2004**, *60*, 611.
[8] M. E. Tuttolomondo, A. Navarro, E. L. Varetti, A. Ben Altabef, *J. Raman Spectrosc.* **2005**, *36*, 427.
[9] M. F. Erben, C. O. Della Vedova, R. Boese, H. Willner, C. Leibold, H. Oberhammer, *Inorg. Chem.* **2003**, *42*, 7297.
[10] J. S. Binkley, J. A. Pople, W. J. Hehre, *J. Am. Chem. Soc.* **1980**, *102*, 939.

[11] M. S. Gordon, J. S. Binkley, J. A. Pople, W. J. Pietro, W. J. Hehre, *J. Am. Chem. Soc.* **1982**, *104*, 2797.
[12] W. J. Pietro, M. M. Francl, W. J. Hehre, D. J. DeFrees, J. A. Pople, J. S. Binkley, *J. Am. Chem. Soc.* **1982**, *104*, 5039.
[13] W. J. Hehre, R. Ditchfield, J. A. Pople, *J. Chem. Phys.* **1972**, *56*, 2257.
[14] P. C. Hariharan, J. A. Pople, *Theor. Chim. Acta* **1973**, *28*, 213.
[15] M. S. Gordon, *Chem. Phys. Lett.* **1980**, *76*, 163.
[16] C. Møller, M. S. Plesset, *Phys. Rev.* **1934**, *46*, 618.
[17] C. Lee, W. Yang, R. G. Parr, *Phys. Rev. B* **1988**, *37*, 785; A. D. Becke, *J. Chem. Phys.* **1993**, *98*, 5648.
[18] A. D. Becke, *J. Chem. Phys.* **1996**, *104*, 1040.
[19] A. D. McLean, G. S. Chandler, *J. Chem. Phys.* **1980**, *72*, 5639.
[20] R. Krishnan, J. S. Binkley, R. Seeger, J. A. Pople, *J. Chem. Phys.* **1980**, *72*, 650.
[21] M. J. Frisch, J. A. Pople, J. S. Binkley, *J. Chem. Phys.* **1984**, *80*, 3265.
[22] T. H. Dunning Jr, *J. Chem. Phys.* **1989**, *90*, 1007.
[23] A. Schaefer, H. Huber, R. Ahlrichs, *J. Chem. Phys.* **1994**, *100*, 5829.
[24] F. Weigend, M. Haeser, H. Patzelt, R. Ahlrichs, *Chem. Phys. Lett.* **1998**, *294*, 143.
[25] V. A. Sipachev, *J. Mol. Struct. (THEOCHEM)* **1985**, *121*, 143.
[26] a) N. W. Mitzel, B. A. Smart, A. J. Blake, H. E. Robertson, D. W. H. Rankin, *J. Phys. Chem.* **1996**, *100*, 9339; b) A. J. Blake, P. T. Brain, H. McNab, J. Miller, C. A. Morrison, S. Parsons, D. W. H. Rankin, H. E. Robertson, B. A. Smart, *J. Phys. Chem.* **1996**, *100*, 12280; c) N. W. Mitzel, D. W. H. Rankin, *Dalton Trans.* **2003**, 3650.
[27] C. Leibold, H. Oberhammer, T. D. Thomas, L. J. Saethre, R. Winter, G. L. Gard, *Inorg. Chem.* **2004**, *43*, 3942.
[28] L. E. Fernández, E. L. Varetti, *J. Mol. Struct. (THEOCHEM)* **2003**, *629*, 175.
[29] A. B. Nielsen, A. J. Holder, *GaussView, User's Reference*, Gaussian, Inc., Pittsburgh PA, **1997–1998**.
[30] E. B. Wilson, J. C. Decius, P. C. Cross, *Molecular Vibrations*, McGraw-Hill, New York, **1955**.
[31] G. Fogarasi, X. Zhou, P. W. Taylor, P. Pulay, *J. Am. Chem. Soc.* **1992**, *114*, 8191.
[32] P. Pulay, G. Fogarasi, G. Pongor, J. E. Boggs, A. Vargha, *J. Am. Chem. Soc.* **1983**, *105*, 7037.
[33] F. Kalincsák, G. Pongor, *Spectrochim. Acta Part A* **2002**, *58*, 999.
[34] W. B. Collier, *Program FCARTP (QCPE # 631)*, Department of Chemistry, Oral Roberts University, Tulsa OK, USA, **1992**.
[35] C. M. Huntley, G. S. Laurenson, D. W. H. Rankin, *J. Chem. Soc., Dalton Trans.* **1980**, 954.
[36] H. Fleischer, D. A. Wann, S. L. Hinchley, K. B. Borisenko, J. R. Lewis, R. J. Mawhorter, H. E. Robertson, D. W. H. Rankin, *Dalton Trans.* **2005**, 3221.
[37] S. L. Hinchley, H. E. Robertson, K. B. Borisenko, A. R. Turner, B. F. Johnston, D. W. H. Rankin, M. Ahmadian, J. N. Jones, A. H. Cowley, *Dalton Trans.* **2004**, 2469.
[38] A. W. Ross, M. Fink, R. Hilderbrandt, *International Tables for Crystallography Vol. C* (Ed.: A. J. C. Wilson), Kluwer Academic Publishers, Dordrecht, Boston and London, **1992**, p. 245.
[39] *Parallel Quantum Solutions*, Fayetteville AR, USA.
[40] M. J. Frisch, G. W. Trucks, H. B. Schlegel, G. E. Scuseria, M. A. Robb, J. R. Cheeseman, J. A. Montgomery Jr, T. Vreven, K. N. Kudin, J. C. Burant, J. M. Millam, S. S. Iyengar, J. Tomasi, V. Barone, B. Mennucci, M. Cossi, G. Scalmani, N. Rega, G. A. Petersson, H. Nakatsuji, M. Hada, M. Ehara, K. Toyota, R. Fukuda, J. Hasegawa, M. Ishida, T. Nakajima, Y. Honda, O. Kitao, H. Nakai, M. Klene, X. Li, J. E. Knox, H. P. Hratchian, J. B. Cross, C. Adamo, J. Jaramillo, R. Gomperts, R. E. Stratmann, O. Yazyev, A. J. Austin, R. Cammi, C. Pomelli, J. W. Ochterski, P. Y. Ayala, K. Morokuma, G. A. Voth, P. Salvador, J. J. Dannenberg, V. G. Zakrzewski, S. Dapprich, A. D. Daniels, M. C. Strain, O. Farkas, D. K. Malick, A. D. Rabuck, K. Raghavachari, J. B. Foresman, J. V. Ortiz, Q. Cui, A. G. Baboul, S. Clifford, J. Cioslowski, B. B. Stefanov, G. Liu, A. Liashenko, P. Piskorz, I. Komaromi, R. L. Martin, D. J. Fox, T. Keith, M. A. Al-Laham, C. Y. Peng, A. Nanayakkara, M. Challacombe, P. M. W. Gill, B. Johnson, W. Chen, M. W. Wong, C. Gonzalez, J. A. Pople, *Gaussian 03, Revision B.02*, Gaussian Inc., Pittsburgh PA, **2003**.
[41] EPSRC National Service for Computational Chemistry Software. URL: http://www.nsccs.ac.uk.

Received: October 4, 2006
Published Online: February 21, 2007

